



Full length article

Chemical modification of TiO₂ nanotube arrays for label-free optical biosensing applications

Monica Terracciano^a, Vardan Galstyan^{b,c}, Ilaria Rea^a, Maurizio Casalino^a, Luca De Stefano^{a,*}, Giorgio Sberveglieri^b

^a Institute for Microelectronics and Microsystems, National Research Council, Via P. Castellino 111, 80131, Naples, Italy

^b Sensor Lab, CNR-INO and Department of Information Engineering, University of Brescia, Via Valotti 9, 25133 Brescia, Italy

^c Department of Molecular and Translational Medicine, University of Brescia, Viale Europa 11, 25123 Brescia, Italy

ARTICLE INFO

Article history:

Received 21 March 2017

Received in revised form 27 April 2017

Accepted 3 May 2017

Available online 4 May 2017

Keywords:

TiO₂ nanotubes surface functionalization

Protein A

Interferometry

Photoluminescence

Bio-sensing

ABSTRACT

In this study, we have fabricated TiO₂ nanotube arrays by the potentiostatic anodic oxidation of Ti foils in fluoride-containing electrolyte and explored them as versatile devices for biosensing applications. TiO₂ nanotubes have been chemically modified in order to bind Protein A as a specific target analyte for the optical biosensing. The obtained structures have been characterized by scanning electron microscopy, Fourier transform infrared spectroscopy, water contact angle, fluorescence microscopy, spectroscopic reflectometry and photoluminescence. Investigations show that the prepared TiO₂ nanotubes, 2.5 μm long and 75 nm thick, can be easily and efficiently bio-modified, and the obtained structures are strongly photoluminescent, thus suitable for the label-free biosensing applications in the range of μM, due to their peculiar optical properties.

© 2017 Elsevier B.V. All rights reserved.

1. Introduction

A growing demand of fast, efficient, low-cost and portable devices for real-time detection of specific analyte has meant biosensing one of the most rapidly expanding research field [1]. The term "biosensor" refers to an integrated receptor-transducer device able of providing selective analytical information by using biological recognition element (i.e., bioprobe). The transducer converts the changes caused by the reaction between the bioprobe and the target into an analytical signal, depending on the technology used [2]. Over the last two decades, several types of electrochemical, optical or electrical biosensors have been developed, resulting valid label-free analytical tools for clinical diagnostics, biomedicine, environmental monitoring, veterinary and food quality control and other areas in which fast and reliable analysis are needed [3]. Titanium dioxide (TiO₂) is a widely studied non-toxic semiconductor and has been investigated as potential transducer material for sensing application due to its unique physicochemical properties [4–7]. It has been observed that the properties of TiO₂ can be enhanced by the nanoscale architectural features [8]: Lu and co-workers

demonstrated that the anatase TiO₂ nanosheets show higher photocatalytic activity for the degradation of organic molecules than anatase TiO₂ crystals [9]. These results encouraged the material science research to focus mainly on nanostructured TiO₂. Recently it was demonstrated that the TiO₂ nanotube arrays directly grown on metallic titanium foil by means of electrochemical anodization are very attractive functional materials in the design of biosensors for biomedical applications owing their high surface area, large refractive index ($n=2.5$), high orientation and uniformity, as well as the good biocompatibility, great aqueous and chemical stability [10,11]. Herein, we fabricated TiO₂ nanotubes (NTs) by means of electrochemical anodization and investigated the prepared samples as the platform for label-free optical monitoring of biomolecules. The use of TiO₂ NT in biosensor development as a transducer surface, required the creation of coupling points for the immobilization of biomolecules (the so-called bioconjugation process), preserving the specific functionalities of biological receptors through a good control of their orientation and organization on the inorganic surface [12]. To this aim, the surface of nanostructured titania was chemically modified in order to covalently bind the protein A by using the well-known silane and silanol chemistries [13,14]. Protein A immobilization was monitored by the optical methods based on the spectroscopic reflectometry and the steady-state photoluminescence. Our results show that the TiO₂ NTs can be

* Corresponding author.

E-mail addresses: luca.destefano@cnr.it, [\(L. De Stefano\)](mailto:luca.destefano@na.imm.cnr.it).

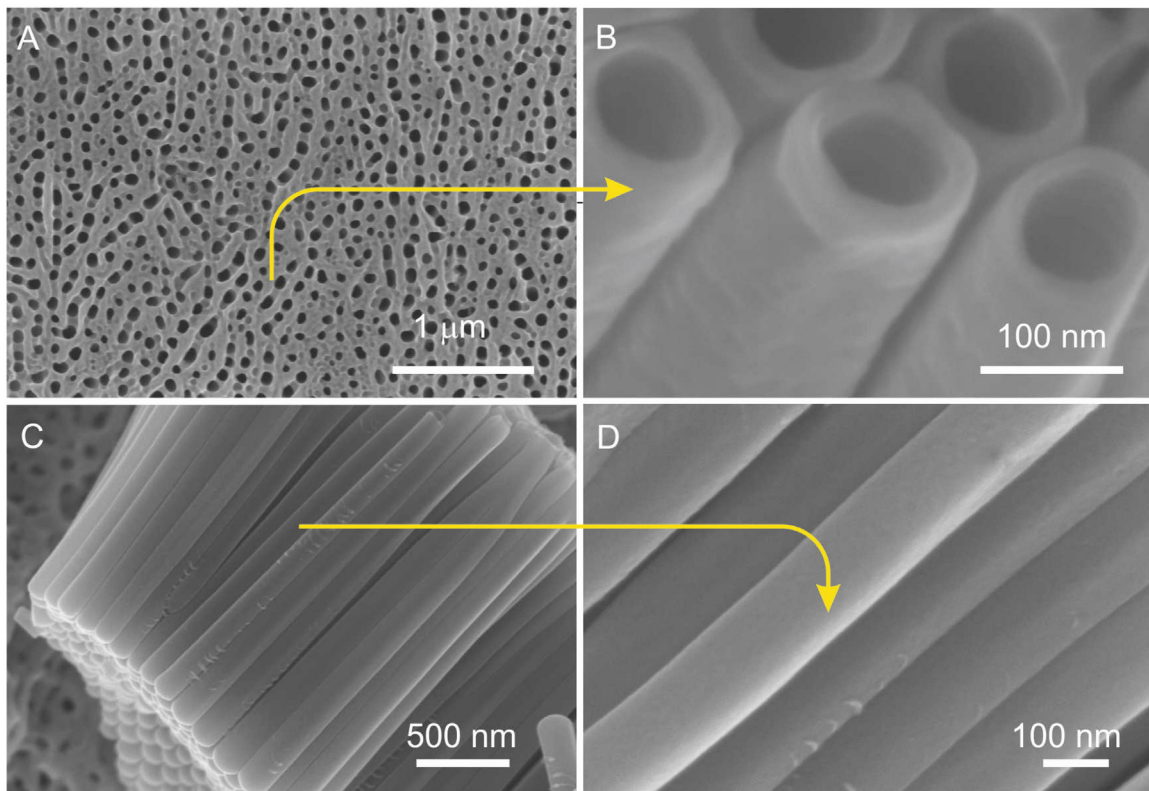


Fig. 1. SEM images of the obtained TiO_2 NTs: (A) and (B) surface morphologies of the nanotube arrays with the different resolutions, (C) and (D) cross-sectional view of the nanotubes with the different resolutions.

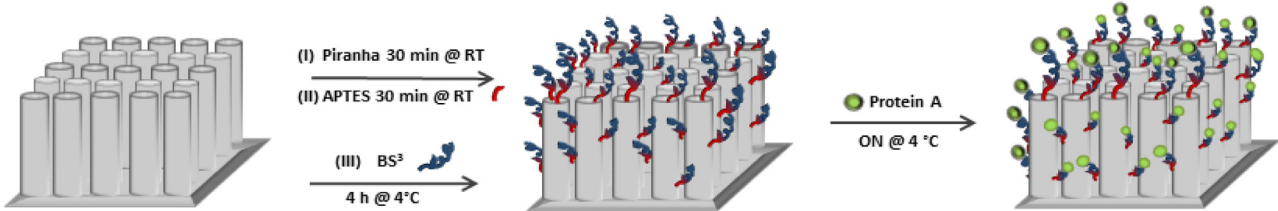


Fig. 2. Schematic representation of the TiO_2 NTs functionalization with Protein A.

applied as versatile platform for sensing of biochemical molecules based on two different optical methods.

2. Experimental

2.1. Fabrication and functionalization of TiO_2 nanotubes

TiO_2 NTs were fabricated by means of electrochemical anodization performed in the electrochemical cell with the two-electrode system. Pt foil was used as a counter electrode. The metallic foils were anodized in NH_4F and H_2O containing glycerol. The anodization was carried out by potentiostatic mode at room temperature. After anodization the prepared samples were washed in distilled water and dried at room temperature. Then, as-prepared NTs were crystallized in the anatase structure using the thermal treatment regimens reported in our previous study [15,16]. The surface of TiO_2 NTs was first activated by Piranha solution (H_2O_2 : H_2SO_4 1:4) for 30 min, in order to create OH groups. Then, the samples were extensively washed in milli-Q water to remove any adsorbed acid on the surface. The structures were silanized by immersion in 5% 3-aminopropyltriethoxysilane (APT) solution in anhydrous toluene for 30 min at room temperature [13]. The prepared samples were

rinsed in toluene three times for 2 min to remove silane excess. Afterwards, the silane was cured on the heater at 100 °C for 10 min. Fluorescein isothiocyanate (FITC) was used to attach a fluorescent label to Protein A (PrA, MW 42 kDa). The labelled Protein A (PrA*) and the not labelled protein A (PrA) were immobilized on the surface of TiO_2 NT arrays using bis(sulfosuccinimidyl)suberate (BS³) crosslinker [13]. The scheme of samples' functionalization process is reported in Fig. 2. The obtained samples were incubated with 150 μl of 1.6 mM BS³ in PBS solution (0.1 M; pH = 7.4) at 4 °C for 4 h. N-hydroxysulfosuccinimide (NHS) ester reacts (through SN2) with primary amines of silanized surface forming stable amine bonds and releasing a NHS group. Then, the functionalized samples were incubated overnight (ON) at 4 °C with 150 μl of 2 mg/ml PrA in PBS (0.1 M; pH = 7.4) buffer. NHS ester reacted with primary amines in the side chain of lysine residues of PrA forming stable amine bonds and releasing another NHS group. The chemicals and the solvents used for the experiments were purchased from Sigma-Aldrich.

2.2. Analyses of the samples

The morphologies of the obtained NTs were analyzed using LEO 1525 scanning electron microscope (SEM) equipped with

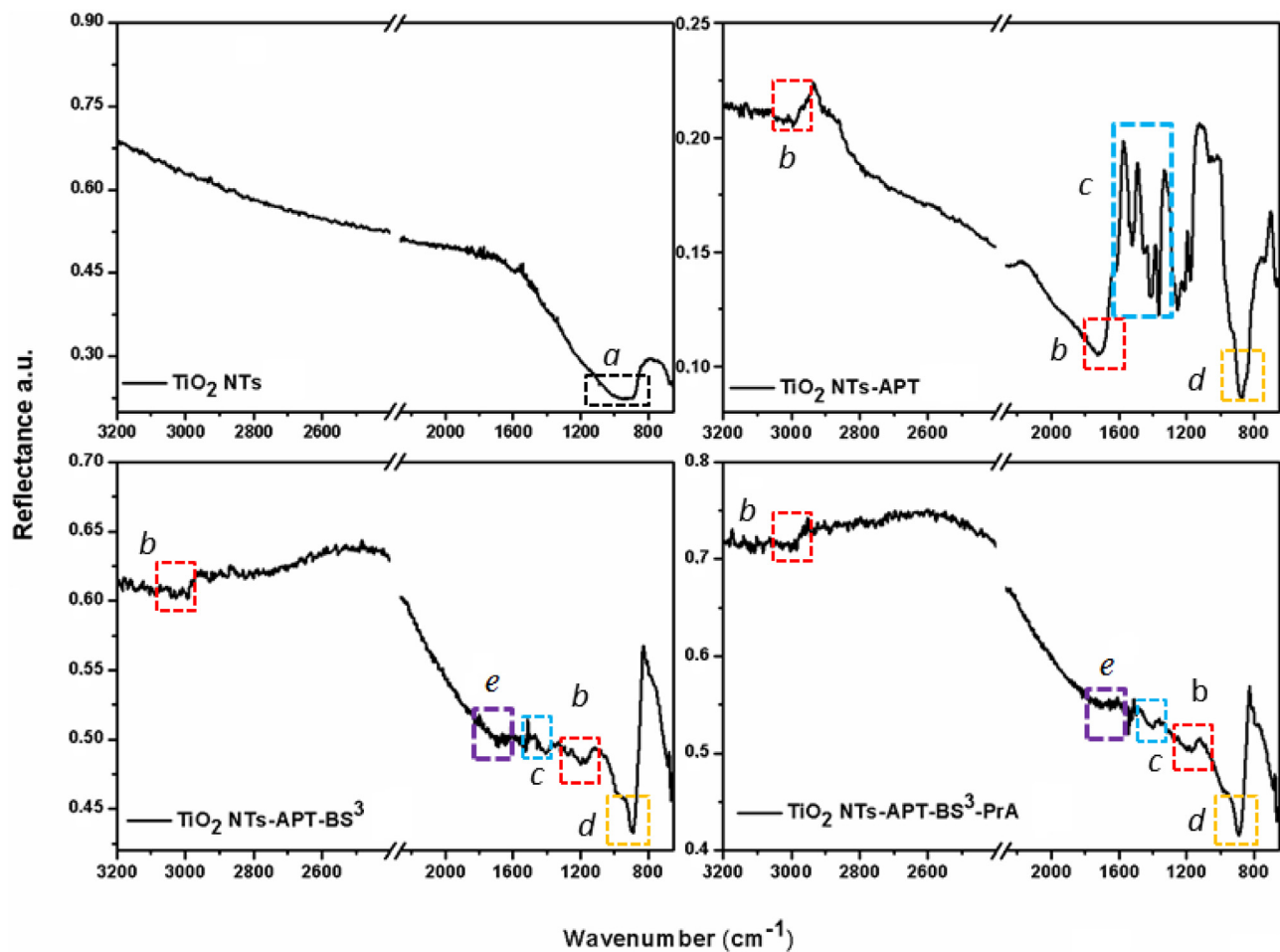


Fig. 3. FTIR spectra of TiO_2 NTs after each step of functionalization: **a** indicates $\text{Ti}-\text{O}-\text{Ti}$ bond, **b** CH_x stretching vibration, **c** the bending mode of the free NH_2 and the $\text{C}-\text{N}$ stretching, **e** $\text{C}=\text{O}$ stretching vibration, **d** the rocking CH_x vibration, respectively.

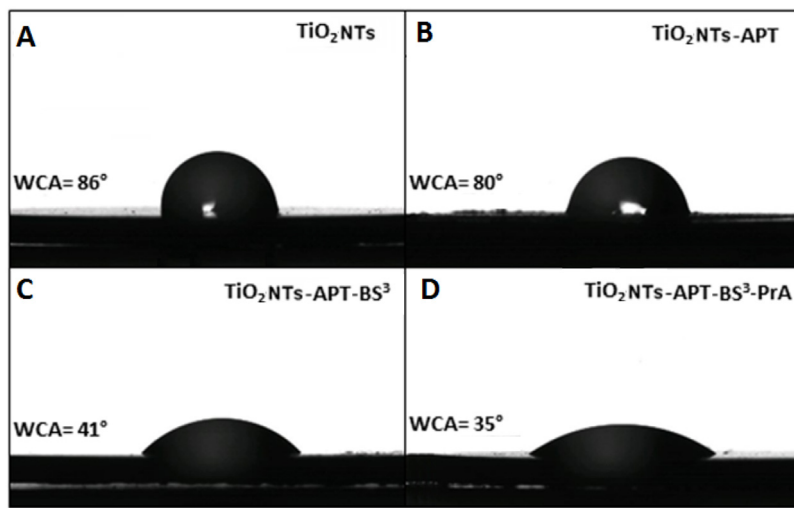


Fig. 4. Water contact angle measurements performed on TiO_2 NTs before and after each step of functionalization.

field emission gun. The chemical composition of TiO_2 NTs before and after surface modification was investigated by Fourier transform infrared spectroscopy (FTIR) spectra. The Fourier transform infrared spectra of all samples were obtained using a Nicolet Continuum XL (Thermo Scientific) microscope in the wavenumber region of $4000\text{--}650\text{ cm}^{-1}$ with a resolution of 2 cm^{-1} . Sessile

drop technique was used for the water contact angle (WCA) measurements on the First Ten Angstroms FTA 1000C Class coupled with drop shape analysis software. The WCA values reported in this work are the average of at least three measurements.

A Leica Z16 APO fluorescence microscope equipped with a Leica camera DFC320 was used to evaluate the bioconjugation of TiO_2

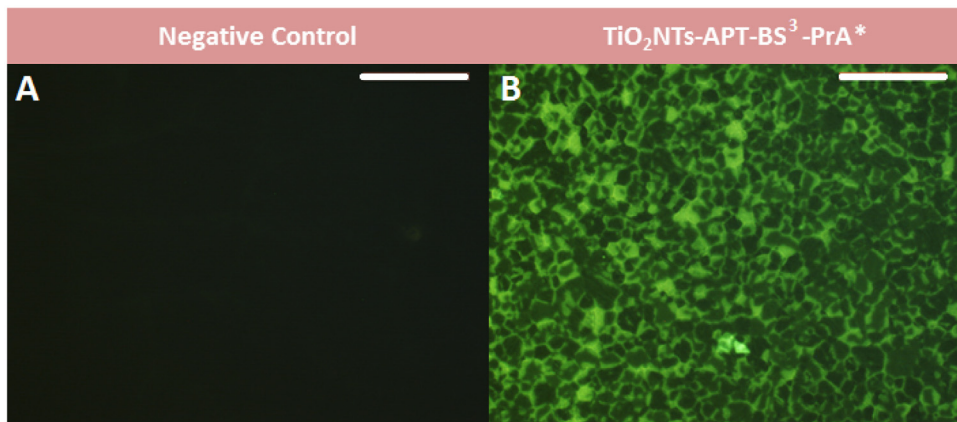


Fig. 5. Fluorescence characterization of the negative control (A) and TiO_2 NTs-APT-BS³ (B) after the incubation with the solutions containing Protein A*. Scale bar, 100 μm .

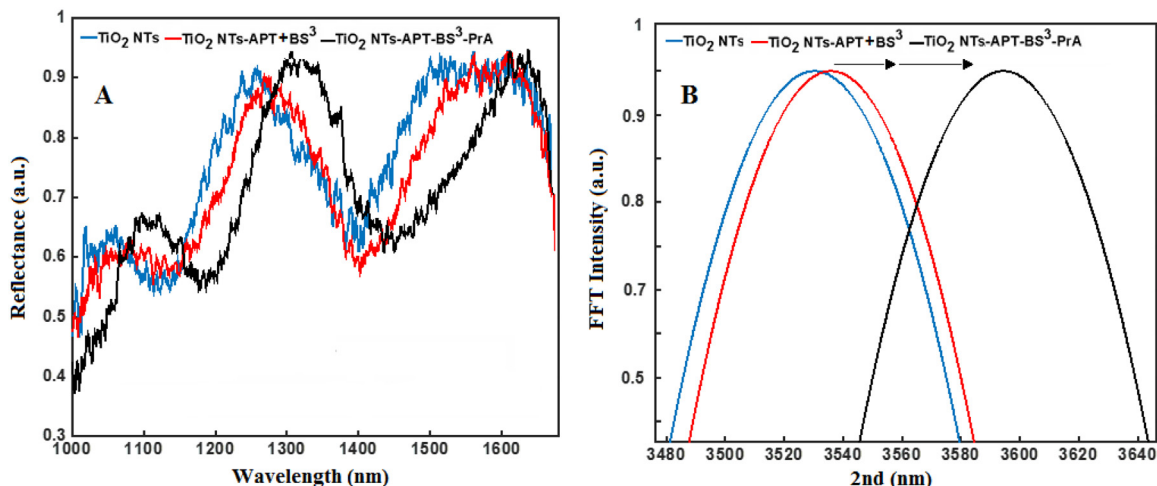


Fig. 6. Reflectivity spectra (A) and corresponding Fourier transforms (B) of TiO_2 NTs before (blue line), after APT+ BS3 (red line) and after PrA (black line). (For interpretation of the references to colour in this figure legend, the reader is referred to the web version of this article.)

NTs with PrA*. The filter used for the acquisition was I3 consisting of a 450–490 nm band-pass excitation filter, a 510 nm dichromatic mirror and a 515 nm suppression filter. Reflectivity spectra of TiO_2 NTs were acquired before and after the functionalizations by a simple experimental setup: a white light was sent on PSi through a Y optical fiber (Avantes). The same fiber was used to guide the output signal to an optical spectrum analyser (Ando AQ6315A). The spectra were acquired at normal incidence over the range from 800 to 1600 nm with a resolution of 5 nm. Reflectivity spectra reported in the work are the average of three measurements. Steady-state photoluminescence (PL) spectra before and after TiO_2 NTs surface functionalization were excited by a continuous wave He–Cd laser at 325 nm (KIMMON Laser System). PL was collected at normal incidence to the surface of samples through a fiber, dispersed in a spectrometer (Princeton Instruments, SpectraPro 300i), and detected using a Peltier cooled charge coupled device (CCD) camera (PIXIS 100F). A long pass filter with a nominal cut-on wavelength of 350 nm was used to remove the laser line at monochromator inlet.

3. Results and discussion

Fig. 1 shows the SEM images of the prepared TiO_2 NTs. The surface (**Fig. 1(A)** and (**B**)) and the cross-sectional (**Fig. 1(C)** and (**D**)) morphological analyses of the samples show that were obtained well-aligned and highly ordered TiO_2 NTs with the inner diameter of 75 nm and the length of 2.5 μm . In order to fabricate

biosensors based on prepared TiO_2 NTs, the material was firstly hydroxylated by Piranha solution (**Fig. 2, I**) Thus, increasing the reactivity of TiO_2 surface by the introduction of –OH groups and making it able to graft alkylsilane molecules of APT (**Fig. 2, II**) [13]. Alkylsilane strategy generated self-assembled monolayers with well-defined packing. The formation of covalent Ti–O–Si bonds between hydroxyl group induced on TiO_2 NTs surface and hydrolyzed organosilane molecules, improves the surface stability and introduces coupling points (–NH₂ groups) for the immobilization of amino-terminated bioprobes [17]. Protein A (PrA), derived from *Staphylococcus aureus* bacteria, is a part of a small collection of proteins known to specifically bind to the constant domain of a number of antibodies. This protein was used as specific bio-receptor for the realization of TiO_2 NTs biosensor. Moreover, since PrA is secreted by and displayed on the cell membrane of *S. aureus*, it is an important biomarker for this bacterium. Therefore, its rapid and specific detection facilitate the pathogen identification and initiation of proper treatment [18]. The protein was covalently conjugated to amino-modified surface (TiO_2 NTs-APT) using the crosslinker BS³ (**Fig. 2, III and IV**).

The chemical modification of TiO_2 NTs was analysed by FTIR spectroscopy (**Fig. 3**). FTIR spectrum of bare TiO_2 NTs showed a typical peak of titania at 948 cm^{-1} [19]. After the silanization process, the TiO_2 NTs-APT displayed characteristic bands of APT corresponding to the CH_x stretching at 2960 and 1720 cm^{-1} [20,21], the bending mode of free NH₂ at 1520–1330 cm^{-1} [22,23] and at

870 cm⁻¹ the rocking CH_x vibration of Si–OCH_x bond [20]. After the BS³, the TiO₂ NTsA-APT-BS³ showed the stretching bands of CH_x at 2960–2849 cm⁻¹, the C–H bending vibrations at 1722 cm⁻¹ [20,23], the amide I band at 1640 cm⁻¹ associated with the C=O stretching vibration, the amide II resulting from the C–N stretching vibration at 1360 cm⁻¹. This result confirmed the covalent binding of the BS³ molecule onto TiO₂ NTsA surface [23]. After incubation with the protein, the TiO₂ NTs-APT-BS³-PrA showed bands of CH_x at 2960–2849 cm⁻¹, the C–H bending vibrations at 1722 cm⁻¹ (20, 21), the amide I band at 1640 cm⁻¹ associated with the C=O stretching vibration and the amide II resulting from the C–N stretching vibration at 1360 cm⁻¹. Consequently, confirming the covalent binding of the PrA onto TiO₂ NTs surface [20,23]. The surface wettability (generally referred to as hydrophobicity/hydrophilicity) plays a key role for the development of biosensors affecting surface bio-functionalization, biomolecular interaction and consequent target recognition [24]. The variation of surface wettability of TiO₂ NTs before and after each step of functionalization processes was characterized by measurements of WCA, as shown in Fig. 4. The TiO₂ NTs are quasi hydrophobic (Fig. 4A), resulting in a WCA value of (86 ± 3)°. APT, with its amino-terminal alkyl chain induces a weak decrease of the WCA to (80 ± 1)° (Fig. 4B). BS³, due to the introduction on the surface of hydrophilic N-hydroxysulfosuccinimide groups (NHS), decreases the WCA down to (41 ± 6)°, thus making the sample surface more hydrophilic than before and therefore suitable for PrA bioconjugation (Fig. 4C). The bioconjugation of TiO₂ NTsA device to PrA was confirmed by a further decrease of WCA value to (35 ± 2)° due to the hydrophilic nature of the protein. The biofunctionalization of TiO₂ NTs with the PrA has been monitored by spectroscopic reflectometry (Fig. 5). To compare the results, the samples were also monitored by the fluorescence microscopy (Fig. 6).

The optical thickness (OT) of the obtained TiO₂ NTs device was calculated from the reflectivity spectrum by FFT, which displayed a peak whose position along the x-axis corresponded to two times the optical thickness (2OT) of the layer [25]. Normal incidence reflectivity spectra of TiO₂ NTs before and after APT + BS³ modification (TiO₂ NTsA-APT-BS³) and after the functionalization with the PrA (TiO₂ NTsA-APT-BS³-PrA) are shown in Fig. 5 together with the corresponding FFTs (Fig. 5B). Since the physical thickness *d* of the TiO₂ NTs layer was fixed, the FFT peak shift of about 10 nm after APT + BS³ and 50 nm after PrA was really due to an increase of the average refractive index (*n*), i.e. more matter in the pores, which was the confirmation of a successful bio-functionalization [17]. In Fig. 6 are reported the fluorescence images of negative control (Fig. 6A) and TiO₂ NTsA-APT-BS³ after incubation with the PrA* (Fig. 6B). The TiO₂ NTs-APT-BS³-PrA* showed a high green fluorescence, contrary to the dark negative control, confirming the bio-conjugation of the biological molecule to surface device.

Steady-state PL spectra of TiO₂ NTs before and after each functionalization step are reported in Fig. 7. TiO₂ NTs showed a PL peak at about 390 nm corresponding to 3.2 eV which is well matched with the band gap energy of anatase TiO₂ [26,27]. The broad visible emission is due to recombination of oppositely charge-carriers at defect energy levels. In the visible region of spectrum is well evident that the PL emission increased after each functionalization step of TiO₂ NTsA surface. This feature is due to the extra free electrons supplied by the molecular complexes (i.e. APT, BS³, PrA), which participated to excitation-relaxation dynamic between the surface energy levels. This phenomenon was less evident in case of the peak at 390 nm, since this last was due to the radiative transitions between conduction and valence bands that were not affected by functionalization treatments. It must be mentioned that TiO₂ NT arrays are excellent photocatalyst for light degradation of many substances [26], but in the presented case, the chemical passiva-

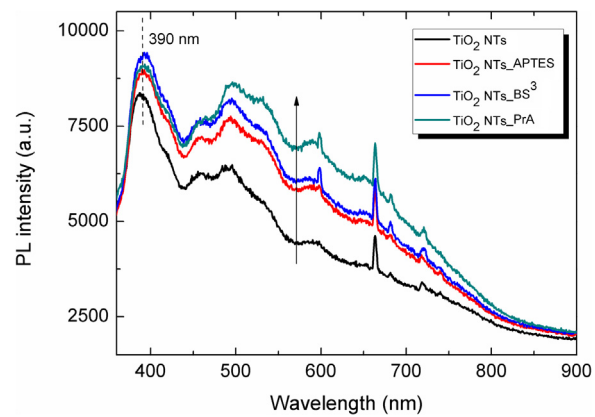


Fig. 7. Photoluminescence spectra changes of TiO₂ NTs after each step of functionalization.

tion of titania nanotubes surface, due to the organic layers added (APT ± BS³), created enough distance between the biological active molecule (PrA) and the photocatalytic titania surface so that protein degradation was prevented.

4. Conclusions

In summary, we fabricated and investigated the properties of TiO₂ NTs for their application in biosensor devices. In order to develop biosensor based on TiO₂ NT arrays the obtained devices were grafted by APT alkylsilane compound, providing coupling points to immobilize the bioprobe, and then bioconjugated to PrA via BS³ molecule. The device bio-functionalization was confirmed qualitatively and quantitatively by several complementary techniques, such as FTIR spectroscopy, WCA measurements, fluorescence microscopy, and label-free optical methods based on spectroscopic reflectometry followed by FFT and PL analysis. PrA was covalently grafted on TiO₂ NTs surface in the range of μM and monitored as a large variation in the PL intensity (more than 1000 a.u) with a corresponding increase of the optical thickness of the sample (about 50 nm). In a label-free optical biosensing experiment, a primary antibody of PrA should be immobilized and used as the bio-probe, and the optical response in binding to PrA should be monitored. Many photoelectrochemical (PEC) sensors using TiO₂ nanotubes array have been reported in literature [29–31], some of them showing very high sensitivity. Even if very sensitive, PEC sensors often require extra decoration of nanotubes (by polymers or metals) in order to get these performances, and they must use a light source and electrical equipment for signal detection. In our case, the experimental results, even if represented only a proof-of-concept for the application of TiO₂ nanotube arrays as transducer materials, were fabricated and modified by standard and well-established procedures, easily reproducible in other laboratories. Moreover, the experimental setup required only a light source (passive for reflection measurements or active for photoluminescent ones) and simple signal elaboration, making the proposed system very attractive for the development of label-free optical biosensors that could be used for a wide range of applications, from biomedical diagnostic and environmental monitoring to food quality control.

References

- [1] X. Zhang, Q. Guo, D. Cui, Recent advances in nanotechnology applied to biosensors, Sensors 9 (2009) 1033–1053.
- [2] J.J. Gooding, Biosensor technology for detecting biological warfare agents: recent progress and future trends, Anal. Chim. Acta 559 (2006) 137–151.
- [3] N. Golego, S.A. Studenikin, M. Cocivera, Sensor photoresponse of thin-film oxides of zinc and titanium to oxygen gas, J. Electrochem. Soc. 147 (2000) 1592–1594.

- [4] L. Yang, S. Luo, Q. Cai, S. Yao, A review on TiO₂ nanotube arrays: fabrication, properties, and sensing applications, *Sci. Bull.* 55 (2010) 331–338.
- [5] H. Cao, Y. Zhu, L. Tang, X. Yang, C. Li, A glucose biosensor based on immobilization of glucose oxidase into 3D macroporous TiO₂, *Electroanalysis* 20 (2008) 2223–2228.
- [6] S. Wu, Z. Weng, X. Liu, K.W.K. Yeung, P. Chu, Functionalized TiO₂ based nanomaterials for biomedical applications, *Adv. Funct. Mater.* 24 (2014) 5464–5481.
- [7] V. Galstyan, E. Comini, G. Faglia, G. Sberveglieri, TiO₂ Nanotubes: recent advances in synthesis and gas sensing properties, *Sensors* 13 (2013) 14813–14838.
- [8] X.G. Han, Q. Kuang, M.S. Jin, Z.X. Xie, L.S. Zheng, Synthesis of titania nanosheets with a high percentage of exposed (001) facets and related photocatalytic properties, *J Am. Chem. Soc.* 131 (2009) 3152–3153.
- [9] H.G. Yang, C.H. Sun, S.Z. Qiao, J. Zou, G. Liu, S.C. Smith, G.Q. Lu, Anatase TiO₂ single crystals with a large percentage of reactive facets, *Nature* 453 (2008) 638–641.
- [10] K.S. Mun, S.D. Alvarez, W.Y. Choi, M.J. Sailor, A stable, label-free optical interferometric biosensor based on TiO₂ nanotube array, *ACS Nano* 4 (2010) 2070–2076.
- [11] R. Wang, C. Ruan, D. Kanayeva, K. Lassiter, Y. Li, TiO₂ nanowire bundle microelectrode based impedance immunosensor for rapid and sensitive detection of Listeria monocytogenes, *Nano Lett.* 8 (2008) 2625–2631.
- [12] N.K. Chaki, K. Vijayamohanan, Self-assembled monolayers as a tunable platform for biosensor applications, *Biosens. Bioelectron.* 17 (2002) 1–12.
- [13] M. Terracciano, I. Rea, J. Politi, L. De Stefano, Optical characterization of aminosilane-modified silicon dioxide surface for biosensing, *JEOS:RP* 8 (2013) 2573.
- [14] L. De Stefano, G. Oliviero, J. Amato, N. Borbone, G. Piccioli, I. Rea, Aminosilane functionalizations of mesoporous oxidized silicon for oligonucleotide synthesis and detection, *J. R. Soc. Interface* 83 (2013) 20130160.
- [15] V. Galstyan, E. Comini, C. Baratto, A. Ponzoni, M. Ferroni, N. Poli, G. Sberveglieri, Large surface area biphasic titania for chemical sensing, *Sens. Actuator B Chem.* 209 (2015) 1091–1096.
- [16] V. Galstyan, E. Comini, G. Faglia, A. Vomiero, L. Borgese, E. Bontempi, G. Sberveglieri, Fabrication and investigation of gas sensing properties of Nb-doped TiO₂ nanotubular arrays, *Nanotechnology* 23 (2012), <http://dx.doi.org/10.1088/0957-4484/23/23/235706>.
- [17] M. Terracciano, L. De Stefano, N. Borbone, J. Politi, G. Oliviero, F. Nici, I. Rea, Solid phase synthesis of a thrombin binding aptamer on macroporous silica for label free optical quantification of thrombin, *RSC Adv.* 6 (2016) 86762–86769.
- [18] K. Urmann, P. Reich, J.G. Walter, D. Beckmann, E. Segal, T. Scheper, Rapid and label-free detection of protein a by aptamer-tethered porous silicon nanostructures, *J. Biotechnol.* (2017), <http://dx.doi.org/10.1016/j.jbiotec.2017.01.005>.
- [19] X. Sheng, D. Xie, C. Wang, X. Zhang, L. Zhong, Synthesis and characterization of core/shell titanium dioxide nanoparticle/polyacrylate nanocomposite colloidal microspheres, *Colloid Polym. Sci.* 294 (2016) 463–469.
- [20] G. Socrates, *Infrared and Raman Characteristic Group Frequencies/Tables and Charts*, Wiley, Chichester, 2001.
- [21] E.T. Vandenberg, L. Bertilsson, B. Liedberg, K. Uvdal, R. Erlandsson, H. Elwing, I. Lundström, Structure of 3-aminopropyl triethoxy silane on silicon oxide, *J. Colloid Interface Sci.* 147 (1991) 103–118.
- [22] N.M. Martucci, I. Rea, I. Ruggiero, M. Terracciano, L. De Stefano, N. Migliaccio, A. Lamberti, A new strategy for label-free detection of lymphoma cancer cells, *Biomed. Opt. Express* 6 (2015) 1353–1362.
- [23] M. Terracciano, M.A. Shahbaz, A. Correia, I. Rea, A. Lamberti, L. De Stefano, H.A. Santos, Surface bioengineering of diatomite based nanovectors for efficient intracellular uptake and drug delivery, *Nanoscale* 47 (2015) 20063.
- [24] K.L. Mittal, *Contact Angle Wettability and Adhesion*, CRC Press, 2006.
- [25] I. Rea, L. Sansone, M. Terracciano, L. De Stefano, P. Dardano, M. Giordano, M. Casalino, Photoluminescence of graphene oxide infiltrated into mesoporous silicon, *J. Phys. Chem. C* 118 (2014) 27301–27307.
- [26] F. Sannino, P. Pernice, C. Imparato, A. Aronne, G. D'Errico, L. Minieri, D. Pirozzi, Hybrid TiO₂-acetylacetone amorphous gel-derived material with stably adsorbed superoxide radical active in oxidative degradation of organic pollutants, *RSC Adv.* 5 (2015) 93831–93839.
- [27] A. Aronne, M. Fantauzzi, C. Imparato, D. Atzei, L. De Stefano, G. D'Errico, F. Sannino, I. Rea, D. Pirozzi, B. Elsener, P. Pernice, A. Rossi, Electronic properties of TiO₂-based materials characterized by high Ti³⁺ self-doping and low recombination rate of electron-hole pairs, *RSC Adv.* 7 (2017) 2373.
- [28] W.W. Zhao, Z.Y. Ma, D.Y. Yan, J.J. Xu, H.Y. Chen, In situ enzymatic ascorbic acid production as electron donor for CdS quantum dots equipped TiO₂ nanotubes: a general and efficient approach for new photoelectrochemical immunoassay, *Anal. Chem.* 84 (24) (2012) 10518–10521.
- [29] B. Lu, M. Liu, H. Shi, X. Huang, G. Zhao, A novel photoelectrochemical sensor for bisphenol A with high sensitivity and selectivity based on surface molecularly imprinted polypyrrole modified TiO₂ nanotubes, *Electroanalysis* 25 (3) (2013) 771–779.
- [30] C. Ye, M.Q. Wang, Z.F. Gao, Y. Zhang, J.L. Lei, H.Q. Luo, N.B. Li, Ligating dopamine as signal trigger onto the substrate via metal-catalyst-free click chemistry for 'signal-on' photoelectrochemical sensing of ultralow microRNA levels, *Anal. Chem.* 88 (23) (2016) 11444–11449.